p27^{kip1}-dependent gene activity within granulosa cells reveals pathways relevant for control of primordial follicle activation in mice.

Emily R Frost[a,b,c,1], Güneş Taylor[c,1*], Stefan Boeing[d,e], Christophe Galichet[c], Mark A Baker[a,b], Jessie M Sutherland[a,b,2*], Robin Lovell-Badge[c,2*]

[1] These authors contributed equally and should be regarded as co-first authors

[2] These authors contributed equally and should be regarded as co-last authors

[a]School of Biomedical Science & Pharmacy, University of Newcastle, Ring Road, Callaghan, New South Wales, Australia, 2308

[b] Hunter Medical Research Institute, New Lambton Heights, New South Wales, Australia, 2305

[c] Stem Cell Biology and Developmental Genetics Lab, The Francis Crick Institute, London, United Kingdom, NW1 1AT

[d] Bioinformatics and Biostatistics Facility, The Francis Crick Institute, London, United Kingdom, NW1 1AT

[e] Scientific Computing – Digital Development Team, The Francis Crick Institute, London, United Kingdom, NW1 1AT

* Corresponding authors:

Dr Güneş Taylor, Stem Cell Biology and Developmental Genetics Lab, The Francis Crick Institute, London, United Kingdom, NW1 1AT, +447724273535 gunes.taylor@crick.ac.uk

Prof Robin Lovell-Badge, Stem Cell Biology and Developmental Genetics Lab, The Francis Crick Institute, London, United Kingdom, NW1 1AT, +442037961509, robin.lovell-badge@crick.ac.uk

Dr Jessie Sutherland, School of Biomedical Science & Pharmacy, University of Newcastle, Ring Road, Callaghan, New South Wales, Australia, 2308, +61249138735 jessie.sutherland@newcastle.edu.au

This manuscript was deposited in BioRxiv as a preprint (https://doi.org/10.1101/2022.10.24.513438). The copyright holder for this preprint is the author/funder, who has granted bioRxiv a license to display the preprint in perpetuity. It is made available under a CC-BY 4.0 International license.

Classification: Biological Sciences, Developmental Biology

Keywords: ovary, primordial follicle, granulosa cells, cell cycle

Abstract

The number of primordial follicles within the ovary, and their rate of activation, are critical parameters of the female reproductive lifespan. A finite number of primordial follicles are established during early ovarian development when individual oocytes are surrounded by a layer of somatic supporting pregranulosa cells. Primordial follicles remain quiescent until activated and their selective activation represents the definitive first step towards oocyte maturation and ovulation. Activation is characterised by morphological and molecular changes in oocytes and pregranulosa cells, however the cell-type and underlying mechanisms that drive follicle activation are largely unresolved. In this study, we report a single-cell RNA sequencing (scRNAseq) dataset to examine primordial follicle formation and activation. We find that pregranulosa cells undergoing follicle activation are characterised by the expression of several genes previously linked with mature granulosa cells as well several novel candidates: *Tnni3*, *Slc18a2*, *Fam13a* and *Htra1*. Using a combinatorial transcriptomic approach, we utilise a $p27^{kip1}$-null (*Cdkn1b*$^{-/-}$) mouse line to relate this gene expression signature to pregranulosa cells of primordial follicles undergoing activation. This study confirms pregranulosa cell changes drive primordial follicle activation and implies that the cell-cycle regulator $p27^{kip1}$ functions as an early responder within the molecular mechanisms regulating activation.

Significance statement

The number of ovarian primordial follicles, each containing an oocyte, is finite. Therefore their activation rate for eventual ovulation is critical to the female reproductive lifespan. However, the cell types and molecular mechanisms driving activation are unknown. Loss of cell-cycle regulator $p27^{kip1}$ results in over-activation of all primordial follicles in neonatal mice, rapidly resulting in total sterility. Using a combinatorial transcriptomics approach, we define a genetic signature within the supporting pregranulosa cells undergoing follicle activation. We also find transcriptional changes in pregranulosa cells lacking $p27^{kip1}$occur before changes in their morphology associated with activation. Together, these findings confirm

precocious maturation of pregranulosa cells drives primordial follicle activation, and place p27^{kip1} as an important regulator of this supporting cell maturation.

Introduction

The finite number of quiescent primordial follicles within the ovaries and the rate of primordial follicle activation are critical parameters of the female reproductive lifespan. Primordial follicles are formed during gestation and consist of an oocyte with a single layer of surrounding pregranulosa cells (1, 2). Upon activation, pregranulosa cells become steroidogenic granulosa cells and remain in close contact with the oocyte, providing structural and metabolic support, until ovulation (3). Though primordial follicles are assembled throughout the ovary initially, follicles within the central ovarian medulla are lost in a wave of activation-induced apoptosis, typically during late foetal development or neonatally in mammals (4). The remaining primordial follicles reside within the outer ovarian cortex and are cyclically activated for apoptosis or the eventual ovulation of mature oocytes after puberty. The establishment of this 'ovarian reserve' of primordial follicles within the ovarian cortex, and their gradual release from it, sustains fertility over several decades in humans and many months in mice (5). While recent advances reveal roles for pathways such as NOTCH, KITL, TGFß and PI3K in regulating the formation of primordial follicles (6-8), the molecular signals initiating follicle activation remain broadly uncharacterised.

While the initial signal triggering activation remains elusive, multiple molecular pathways are involved in the primordial-to-primary follicle transition (9, 10). Key indicators of follicle activation are changes in oocyte size, granulosa cell morphology (from squamous to cuboidal) and re-entry into the cell-cycle (11-14). Changes in the pregranulosa cells precede changes in the oocyte, suggesting that the signal for primordial follicle activation originates from the pregranulosa cells, initiating signalling cascades in the oocyte (15, 16). This is supported by various genetic models in mice, where loss of crucial factors in pregranulosa cells causes dysregulated primordial follicle activation (17-19).

Studies of follicle activation have typically utilised genetically modified mouse models and microarray approaches to explore the expression of gene-driven signals in stimulating or inhibiting primordial follicle activation (reviewed in (10, 20)). The emergence of single-cell RNA sequencing (scRNAseq) permits examination of heterogenous populations such as follicles within the mouse ovary (21). Dissociation protocols suitable for scRNAseq on neonatal mouse ovary have been developed by our lab and others (22, 23) and used to investigate the mechanisms underpinning germ cell nest breakdown and the first wave of primordial follicle activation in mice (6, 23-26). These datasets provide the transcriptomes of oocytes and granulosa cells during ovarian development, with significant overlap of the genes identified in each study. However, they have yet to elucidate the network driving activation of primordial follicles and how this is altered in ovarian infertility.

Primordial follicle activation is also challenging to interrogate due to the asynchronous nature of activation throughout pre-pubertal and adult life. To overcome these challenges, here we leveraged $p27^{kip1}$ null mutant female mice (*Cdkn1b*$^{-/-}$) with accelerated and ubiquitious neonatal follicle activation to capture the distinct transcriptomic signature of pregranulosa cells undergoing activation throughout the entire ovary (17). We then use these data to functionally interrogate a molecular signature of activating pregranulosa cells established using scRNAseq in wildtype ovaries during the first wave of primordial follicle activation. Importantly, transcriptomic analysis of *Cdkn1b*$^{-/-}$ females revealed that this signature of pregranulosa cells undergoing activation was observed precociously at E18.5. This demonstrates the gene expression changes in pregranulosa cells occur prior to the morphological changes associated with follicle activation. This study supports pregranulosa cell maturation as a key driver of primordial follicle activation and integrates cell-cycle regulator, $p27^{kip1}$, within the molecular mechanism driving this pregranulosa cell transition.

Results

Single-cell transcriptomic profiling the mouse ovary through the first wave of primordial follicle activation activation.

To investigate the transcriptional signature of ovarian cells during the first wave of primordial follicle activation, we performed scRNAseq of one mouse ovary at three timepoints. Namely: embryonic day 18.5 (E18.5), when germ cell nest breakdown is initiated to form primordial follicles; post-natal day 4 (PND4), when the initial wave of primordial follicle activation is occurring; and PND7, when populations of activated follicles (termed primary follicles) are present within the ovary (Figure 1A). A single-cell suspension, enriched for the somatic cell compartment, was obtained using a previously described protocol from single ovaries (22). In total, our dataset contained 24,810 cells, with 8,210 cells at E18.5, 7,587 at PND4 and 9,013 cells at PND7 (Table S1). Data from all three timepoints were integrated and uniform manifold approximation and projection (UMAP) analysis was used to assess cell contribution to individual clusters. In total, 18 distinct clusters were found, and the six major cell types present in the ovary across these developmental stages were annotated based on their expression of established cell type specific genetic markers (granulosa cells, mesenchymal cells, oocytes, epithelial cells, immune cells and blood cells) (Figure 1B and Figure S1A). Across all three timepoints, most cells mapped to either the mesenchymal (43%) or granulosa cell (39%) clusters. Five sub-clusters for granulosa (Gc_1 to Gc_5) and six mesenchymal clusters (Mc_1 to Mc_6) were identified. Following the identification of the clusters, pseudo-differential gene expression analysis was performed and the most differentially expressed genes in each cluster were shown in a heatmap (Figure 1C). Given we hypothesise that it is pregranulosa cells that drive primordial follicle activation, we focused our downstream analysis on the granulosa cell clusters.

Identification of a transcriptional signature indicative of the onset of primordial follicle activation within pregranulosa cells.

Of the granulosa cell clusters, cluster Gc_5 consisted of fewer cells with high expression of Pax8 and ribosomal genes, identifying them as similar to the recently

reported Pax8+ supporting-like cells (Figure S1B) (27). Consequently, we focused on clusters Gc_1 through Gc_4 only. When interrogated by timepoint we observed that Gc_1, Gc_2 and Gc_3 clusters were present from E18.5, while Gc_4 only emerged at PND4 (Figure 2A and Figure S1C). The Gc_4 cluster expressed mature granulosa cell marker genes including *Amhr2* and *Hmgcs2,* and showed high expression of proliferation genes (Figure 2A, 2B and 2C). Therefore, we identified Gc_4 as differentiated granulosa cells (11, 28). We classified Gc_1 as an embryonic population of epithelial-derived pregranulosa cells due to their expression of *Gng13* and *Lgas7*, and the decreased cell numbers in Gc_1 between E18.5 and PND7 (Figure 2A and 2B and Figure S1B and S1C) (4, 6, 29, 30). We identified Gc_2 as a population of pregranulosa cells derived from the *Nr5a1*+ somatic cell lineage based on their high expression of *Cdkn1b* and *Foxl2* combined with the low expression of *Hsd3b1* and *Hmgcs2* (Figure 2B) (6). Interestingly, Gc_3 have similar gene expression signatures to Gc_2 (shown by the expression of *Foxl2* and *Hmgcs2* amongst others), but with elevated expression of well-established markers of activated granulosa cells like *Kitl* and *Fst* (Figure 2B) (12, 31). This suggested that Gc_3 is a population of pregranulosa cells that have initiated primordial follicle activation, that we have termed activating pregranulosa cells.

To see the more discrete gene expression changes within Gc_1, Gc_2, Gc_3 and Gc_4, we performed subcluster analysis on only these granulosa cell clusters. This analysis validated the classification of the four clusters, with significant gene overlap between Gc_2, Gc_3 and Gc_4 (Figure S2 and Dataset S1). Interestingly, these shared Gc genes were significantly downregulated in the Gc_1 cluster. To find the genes that are either switched on or off during follicle activation, we performed differential gene expression (DGE) analyses comparing each cluster to the other three Gc clusters (ie Gc_1 vs all other Gc clusters) (32) (Figure S2 and Dataset S1). We found no unique gene markers of Gc_2, Gc_3 or Gc_4, and rather two distinct gene expression dynamics emerged: genes that increase in expression during activation and persist in mature granulosa cells, and genes that decreased upon entry into the activating pregranulosa cell pool.

We define these two expression dynamics as genes 'switched on' during follicle activation and genes 'switched off' to allow follicle activation to proceed. Genes that were 'switched on' were downregulated in Gc_1 and upregulated in at least 50% of Gc_3 cells, with expression at PND4 (Figure S2A and Dataset S1, S2). This gives a list of genes that are progressively upregulated across Gc_2, Gc_3 and Gc_4. This yielded 58 genes, including established pre-granulosa marker genes of primordial follicle activation including *Amh*, *Inha* and *Nr5a2* (Figure 2E). Genes not previously characterised during primordial follicle activation including *Slc18a2*, *Tnni3*, *Fam13a* and *Htra1* are suitable candidates that share similar gene expression profiles to *Amh*, *Inha* and *Nr5a2*, and are representative of cells entering activation. Genes that were 'switched off' were downregulated in Gc_3 and Gc_4 clusters, and showed expression in at least 50% of Gc_2 cells at E18.5 (Figure S2A and Dataset S2). These genes are downregulated in granulosa cells as activation occurs. This specific dynamic was observed in 22 genes, including established markers of early dormant pregranulosa cells *Gng13*, *Lgr5* and *Irx3* (Figure 2F). Two new genes, *Arl6ip1* and *Myl9,* have not previously characterised in primordial follicles and are downregulated during activation in a similar pattern to *Gng13*, *Lgr5* and *Irx3*. Combined, these 80 genes are a signature of pregranulosa cell changes during the first wave of primordial follicle activation.

Examining changes in pregranulosa cell gene expression in a model of accelerated primordial follicle activation

Having identified putative genes involved in pregranulosa cell activation, we next queried these candidate genes in an established model of precocious and simultaneous follicle activation, using *Cdkn1b*$^{-/-}$ (p27^{kip1}) mice. *Cdkn1b*$^{-/-}$ mice show an uncontrolled activation of follicles perinatally, inducing infertility prior to sexual maturation (17, 33). First, we validated that all primordial follicles activate precociously by studying the histology of *Cdkn1b*$^{-/-}$ and control ovaries at PND8. Larger numbers of primary and secondary follicles were observed in *Cdkn1b*$^{-/-}$ ovaries when compared to controls (Figure 3A). As previously reported, no gross histo-morphological differences between *Cdkn1b*$^{-/-}$ and control ovaries were found at E18.5

(Figure 3B) (17). We performed bulk RNA-sequencing of control and *Cdkn1b*$^{-/-}$ ovaries at three time points, E13.5, E18.5 and PND8. We found only 6 differentially expressed genes at E13.5, 1633 genes at E18.5 and 719 genes at PND8 ($p < 0.05$) (Figure S3). The E13.5 data confirmed pregranulosa cell specification was unperturbed by the loss of *Cdkn1b*. Despite gross morphological changes at PND8, E18.5 showed the highest differential expression. Of these E18.5 genes, 1,008 were upregulated and 626 genes were downregulated in *Cdkn1b*$^{-/-}$ ovaries (Figure 3C, Figure S3A and Dataset S3). This suggested that absence of *Cdkn1b* was causing profound gene changes around germ cell nest breakdown and follicle formation.

Since *Cdkn1b* is exclusively expressed in pregranulosa cells in the developing ovary, we hypothesised that pregranulosa cell gene expression was altered in *Cdkn1b*$^{-/-}$ ovaries. Therefore, we overlaid the 1,633 differentially expressed genes in E18.5 *Cdkn1b*$^{-/-}$ ovaries with the scRNAseq gene expression data from Gc_1 to Gc_4 (Figure 3D). This heatmap revealed that the majority of differentially expressed genes in *Cdkn1b*$^{-/-}$ ovaries at E18.5 were expressed in granulosa cell clusters Gc_3 and Gc_4 (Figure 3D). This indicates precocious activation of pregranulosa cells at E18.5 in *Cdkn1b*$^{-/-}$ mice (Figure 3D). To interrogate this further, we compared our new gene expression signature from the scRNAseq (80 genes) with the 1,633 genes altered in *Cdkn1b*$^{-/-}$ ovaries (Figure 3E). We found seven genes (*Tnni3*, *Gja1, Ubash3b*, *Inha*, *Hsd17b1, Hsd3b1* and *Akr1cl*) that are expressed in Gc_3 cells and are differentially upregulated at E18.5 in *Cdkn1b*$^{-/-}$ ovaries when compared to wild-type ovaries (Figure 3E and Dataset S4). Of the 80 genes in our signature of activation, these seven genes are p27^{kip1}-dependent features in both the wild-type and infertile mouse ovary. Strikingly, not all of the activating pregranulosa cell signature genes are altered in *Cdkn1b*$^{-/-}$ *ovaries,* suggesting that it is these seven genes particularly that are dependent on p27^{kip1} regulation for timely activation to promote primordial follicle activation.

Discussion

In this study, we identify a p27-dependent gene signature within the pregranulosa cells undergoing primordial follicle activation within the neonatal mouse ovary. By

utilising single cell RNA-sequencing, we find five distinct clusters of granulosa cells in three stages of development: E18.5, PND4 and PND7. A distinct population of activating pregranulosa cells was seen and their gene expression signiature identified. This pregranulosa-specific gene expression signature during primordial follicle activation includes novel genes *Tnni3* and *Slc18a2*. *Tnni3* has been identified in human granulosa cells of late-stage follicles and genetic variants of *Slc18a2* are associated with polycystic ovary syndrome (34, 35). These targets have been mentioned in pregranulosa cells in another scRNAseq study (6), however we have shown involvement in a mouse model of dysregulated follicle activation. Further work to piece together how these genes function and cooperate with other primordial follicle activation networks is essential.

The genes that showed specific expression in the activating pregranulosa cell cluster were hypothesised to control follicle activation. To functionally interrogate this hypothesis, we utilised the *Cdkn1b*$^{-/-}$ mouse line that has an accelerated primordial follicle activation phenotype in the neonatal mouse ovary. Contrary to previous reports, transcriptomic analysis of these ovaries revealed distinct gene expression changes as early as E18.5 and preceed any morphological or histological changes in the mutants. Genes upregulated in *Cdkn1b*$^{-/-}$ ovaries were part of the novel gene expression signature of activating pre-granulosa cells identified in our scRNAseq data. While the combination of single cell RNA-sequencing data with bulk RNA-sequencing supports and strengthens our characterisation of the genes involved in primordial follicle activation, to date, this is an under-utilised approach. However, there are important considerations, namely that the bulk sequencing dataset is from a heterogenous mix of ovarian cell types and the sequencing depths of the two technologies are mis-matched. However, this comparison has been shown to be informative in studies on embryonic somatic gonadal cells (36). Of note, it remains to be elucidated if these changes are primarily due to the loss of a cell cycle inhibitor or alternatively, a downstream effect of increased activation due to the direct role of p27^{kip1} in transcriptional repression of specific genes (37). Stringent experiments using inducible *Cdkn1b* gene deletion or overexpression of alternate cell cycle inhibitors may reveal the importance of cell cycle regulators in the developing ovary.

Where the focus is usually on the oocyte, the transcriptomic datasets we provide here highlight the importance and role of somatic cells in follicle activation. Combining this dataset with previously published single cell RNA-sequencing studies of the developing ovary could establish a time course of gene expression across the processes of germ cell nest breakdown, primordial follicle formation and activation, particularly since each study covers different timepoints (6, 7, 23-26, 38). Exciting opportunities also exist to correlate this data with human ovary single cell RNA-sequencing studies and those from other species to uncover how well the process is conserved (39). While our focus was on identifying granulosa cell initiators of follicle activation, opportunities exist to further analyse other cell types captured within this dataset e.g. oocytes, mesenchymal and immune cells.

Questions remain as to whether the loss of cell cycle inhibition in pregranulosa cells solely drives the precocious primordial follicle activation in *Cdkn1b*$^{-/-}$ mutants. In this study, the phenotype of *Cdkn1b*$^{-/-}$ mutants might be exacerbated by the loss of p27^{kip1} in the oocytes, where expression comes on postnatally in wild-type ovaries. A conditional approach deleting *Cdkn1b* in pregranulosa cells specifically, would provide a clear answer if primordial follicle activation is initiated in the pregranulosa cells and dysregulated by the absence of p27^{kip1}. Regardless, it is clear from this body of work that further interrogation is necessary to find the master regulators of follicle activation. The hierarchy of the numerous factors that cause follicle activation are still being explored: as most previous studies have used single gene-deletion models, which makes the construction of a gene regulatory network challenging (9, 40). For p27^{kip1}, potential upstream regulators that may initiate primordial follicle activation by reducing p27^{kip1} expression include FOXL2, WNT4, SMAD2 and JAK2 (41-45). Additionally, given that spatial and temporal control of activation is required to selectively activate follicles in adulthood, epigenetic mechanisms and chromatin accessibility are two unexplored areas that may provide the precise control necessary to activate multiple factors simultaneously. Future experiments using ChIP-sequencing and ATAC-sequencing on pregranulosa cells during the window of activation in the mouse will yield insights into how the genes upregulated during primordial follicle activation are controlled.

In conclusion, this study describes and explores transcriptomic datasets to interrogate primordial follicle activation in the mouse. We reveal a gene expression signature within pregranulosa cells that are undergoing primordial follicle activation and highlight $p27^{kip1}$-dependent genes within this signature. We provide evidence that these transcriptomic changes occur specifically within the pregranulosa cells, and not the oocytes, and that this underpins the molecular mechanism allowing the activation of primordial follicles. We hypothesise that our gene expression signature is a critical part of the molecular control initiating and driving follicle activation. This dataset will be a valuable resource for the interrogation of mammalian follicle activation.

Materials and Methods

Mice

All experiments carried out on mice were approved under the UK Animal (scientific procedures) Act 1986 (Project license 70/8560). Animals were kept in individually ventilated cages (IVC) with access to food and water *ad libitum*. C57BL/6J mice (RRID: IMSR_JAX:000664) were supplied by the Biological Research Facility at the Francis Crick Institute and used for the single-cell sequencing experiments. *Cdkn1b*^{tm1Mlf} (*Cdkn1b*$^{-/-}$) (RRID: IMSR_JAX:002781) (46) were maintained on a mixed background and mated heterozygously. Experiments involving *Cdkn1b*$^{-/-}$ mice were performed using littermate animals (*Cdkn1b*$^{+/+}$*)* as controls.

RNA sequencing sample preparation

Tissue dissociation and single-cell library preparation

Female ovaries at E18.5, PND4 and PND7 were harvested and ovarian tissue was dissociated as previously described (22). Briefly, two ovaries from each timepoint were incubated separately in a solution of papain for 15min at 37°C in presence of 10µg/ml of both DNAse I and Rock Inhibitor (47). The papain solution containing the cells was diluted with 1x HBSS containing 0.0025% BSA and 0.01% 1M Tris pH8.0. The cell solution was then mechanically dissociated using a 10mL glass serological pipette and passed through a 20 µm pre-separation filter. Approximately 10,000 live cells were used to generate libraries using the Chromium Single Cell 3' kit v3.1, according to the manufacturer's instructions (48). The libraries were quantified using

the TapeStation (Agilent) to confirm quantity and purity, before sequencing on an Hiseq4000 (Illumina). Sequencing outputs were processed using the 10x CellRanger (version.3.0.2) to generate single-cell count data for each time point, using a mouse reference index provided by 10x Genomics (refdata-cellranger-mm10v3.0). All subsequent analyses were performed in R v.3.6.0 using the Seurat (v3) package (49).

Data availability

The data supporting the findings of this study are available in the main text and the supplementary materials. Datasets have been submitted to NCBI GEO (Awaiting confirmation of GEO Series ID).

Tissue dissociation and bulk library preparation

Ovaries from *Cdkn1b*$^{+/+}$ and *Cdkn1b*$^{-/-}$ mice were collected at E13.5, E18.5 and PND8. A single ovary was dissociated as described above. RNA was extracted from the dissociated cells using the RNeasy Plus Micro kit (Qiagen) according to the manufacturer's protocol. RNA quality was assessed the TapeStation (Agilent). Libraries were constructed using the NEBNext Low Input RNA Library Prep Kit (E6420L, New England Biolabs) according to the manufacturer's instructions. All libraries were quantified using the TapeStation (Agilent) and sequenced on an Hiseq400 (Illumina) to achieve an average of 25 million reads per sample.

scRNAseq Bioinformatics analysis

Raw single-cell sequencing data from all three timepoints were processed using the 10x CellRanger pipeline (10x Genomics) and analysed with the Seurat package in R (49). All cells with fewer than 1500 RNA features were removed. Principal component analysis was performed on variable genes and 20 principal components were used to generate the UMAP analysis. The UMAP clustering plot was performed using the default method from the Seurat package. Differential Gene Expression (DGE) analysis was performed as previously described (32).

Bulk RNA sequencing analysis

Libraries were sequenced on an Illumina HiSeq 4000 machine. The 'Trim Galore!' utility version 0.4.2 was used to remove sequencing adaptors and to trim individual

reads with the q-parameter set to 20 (https://www.bioinformatics.babraham.ac.uk/projects/trim_galore/). The sequencing reads were then aligned to the mouse genome and transcriptome (Ensembl GRCm38release-89) using RSEM version 1.3.0 (50) in conjunction with the STAR aligner version 2.5.2 (51). The sequencing quality of individual samples was assessed using FASTQC version 0.11.5 (https://www.bioinformatics.babraham.ac.uk/projects/fastqc/) and RNA-SeQC version 1.1.8 (52). Differential gene expression was determined using the R-bioconductor package DESeq2 version 1.14.1 (53, 54).

Histology staining

Ovaries for hematoxylin and eosin (H&E) staining were fixed in chilled 4% (w/v) paraformaldehyde at 4 °C for 1 to 2 hrs. Following fixation, ovaries were washed in PBS 3 times for 1 hr each, before cryoprotection in 30% (w/v) sucrose in PBS overnight. The ovaries were then embedded in OCT mounting medium, frozen on an ethanol/dry ice slurry and stored at -80 °C. Samples were cryosectioned at 10 µm and sections were placed on Superfrost Plus glass slides and air dried for 5 minutes. H&E staining was performed by the Francis Crick Institute Experimental Histopathology facility. H&E images were taken at 10 x magnification and 40 x magnification, with scale bars of 100 µm and 25 µm respectively.

Acknoweldgements and Funding Sources

Acknowledgements

We would like to thank members of the Lovell-Badge and Sutherland laboratories for their comments on the manuscript. We thank the Advanced Sequencing Facility at the Francis Crick Institute for their help in performing the sequencing studies in this manuscript. We acknowledge Biorender software (biorender.com) which was used for the creation of figures. This work was supported by the Francis Crick Institute, which receives its core funding from Cancer Research UK (CC2116), the UK Medical Research Council (CC2116), and the Wellcome Trust (CC2116). We acknowledge the generous financial assistance to R.L.B. by the UK Biotechnology and Biological Sciences Research Council (BB/ N018680/1). We also gratefully acknowledge the

financial assistance to J.M.S. and M.A.B. by the Australian National Health and Medical Research Council (G1600095) and the Hunter Medical Research Institute (G1501433 and G1801335). E.R.F. is the recipient of an Australian Government Research Training Program Scholarship.

Author contributions

G.T. and E.R.F. conceived the study and wrote the manuscript. J.M.S., C.G., M.A.B. and R.L.B. provided expertise and feedback on the study design. All experiments were performed by E.R.F., G.T. and C.G.. RNA-seq and single-cell RNA-seq analyses were performed by S.B.. All the authors critically revised the manuscript. R.L.B. and J.M.S. provided resources for this work.

Declaration of interests

The authors declare no competing interests.

References

1. M. E. Pepling, A. C. Spradling, Mouse ovarian germ cell cysts undergo programmed breakdown to form primordial follicles. *Developmental biology* **234**, 339-351 (2001).
2. C. Tingen, A. Kim, T. K. Woodruff, The primordial pool of follicles and nest breakdown in mammalian ovaries. *Molecular human reproduction* **15**, 795-803 (2009).
3. R. Li, D. F. Albertini, The road to maturation: somatic cell interaction and self-organization of the mammalian oocyte. *Nat. Rev. Mol. Cell Biol.* **14**, 141-152 (2013).
4. W. Zheng *et al.*, Two classes of ovarian primordial follicles exhibit distinct developmental dynamics and physiological functions. *Human molecular genetics* **23**, 920-928 (2014).
5. D. Monniaux *et al.*, The ovarian reserve of primordial follicles and the dynamic reserve of antral growing follicles: what is the link? *Biol. Reprod.* **90**, 85 (2014).

6. W. Niu, A. C. Spradling, Two distinct pathways of pregranulosa cell differentiation support follicle formation in the mouse ovary. *Proceedings of the National Academy of Sciences* **117**, 20015-20026 (2020).
7. J.-J. Wang *et al.*, Single-cell transcriptome landscape of ovarian cells during primordial follicle assembly in mice. *PLoS Biol.* **18**, e3001025 (2020).
8. K. Fukuda, M. Muraoka, Y. Kato, Y. Saga, Decoding the transcriptome of pre-granulosa cells during the formation of primordial follicles in the mouse. *Biol. Reprod.* 10.1093/biolre/ioab065 (2021).
9. D. Adhikari, K. Liu, Molecular mechanisms underlying the activation of mammalian primordial follicles. *Endocrine reviews* **30**, 438-464 (2009).
10. Y. Chen *et al.*, The Factors and Pathways Regulating the Activation of Mammalian Primordial Follicles in vivo. *Frontiers in cell and developmental biology* **8** (2020).
11. K. Hardy *et al.*, Nuclear exclusion of SMAD2/3 in granulosa cells is associated with primordial follicle activation in the mouse ovary. *J. Cell Sci.* **131** (2018).
12. K. J. Hutt, E. A. McLaughlin, M. K. Holland, KIT/KIT Ligand in Mammalian Oogenesis and Folliculogenesis: Roles in Rabbit and Murine Ovarian Follicle Activation and Oocyte Growth1. *Biology of Reproduction* **75**, 421-433 (2006).
13. G. B. John, T. D. Gallardo, L. J. Shirley, D. H. Castrillon, Foxo3 is a PI3K-dependent molecular switch controlling the initiation of oocyte growth. *Developmental biology* **321**, 197-204 (2008).
14. E. R. Frost, G. Taylor, M. A. Baker, R. Lovell-Badge, J. M. Sutherland, Establishing and maintaining fertility: the importance of cell cycle arrest. *Genes Dev.* **35**, 619-634 (2021).
15. S. Lintern-Moore, G. P. Moore, The initiation of follicle and oocyte growth in the mouse ovary. *Biol. Reprod.* **20**, 773-778 (1979).
16. A. Gougeon, G. B. Chainy, Morphometric studies of small follicles in ovaries of women at different ages. *J Reprod Fertil* **81**, 433-442 (1987).
17. S. Rajareddy *et al.*, p27kip1 (cyclin-dependent kinase inhibitor 1B) controls ovarian development by suppressing follicle endowment and activation and

promoting follicle atresia in mice. *Molecular endocrinology (Baltimore, Md.)* **21**, 2189-2202 (2007).

18. M. Uda *et al.*, Foxl2 disruption causes mouse ovarian failure by pervasive blockage of follicle development. *Human molecular genetics* **13**, 1171-1181 (2004).
19. O. Habara, C. Y. Logan, M. Kanai-Azuma, R. Nusse, H. M. Takase, WNT signaling in pre-granulosa cells is required for ovarian folliculogenesis and female fertility. *Development* **148** (2021).
20. A. P. Sobinoff, J. M. Sutherland, E. A. McLaughlin, Intracellular signalling during female gametogenesis. *Molecular human reproduction* **19**, 265-278 (2013).
21. E. R. Frost *et al.*, A New Understanding, Guided by Single-Cell Sequencing, of the Establishment and Maintenance of the Ovarian Reserve in Mammals. *Sex. Dev.* 10.1159/000526426 (2022).
22. E. R. Frost *et al.*, Two alternative methods for the retrieval of somatic cell populations from the mouse ovary. *Mol. Hum. Reprod.* **27** (2021).
23. Y.-Y. Chen *et al.*, Single-cell transcriptomics of staged oocytes and somatic cells reveal novel regulators of follicle activation. *Reproduction* **164**, 55-70 (2022).
24. M.-C. Meinsohn *et al.*, Single-cell sequencing reveals suppressive transcriptional programs regulated by MIS/AMH in neonatal ovaries. *Proceedings of the National Academy of Sciences* **118**, e2100920118 (2021).
25. M. E. Morris *et al.*, A single-cell atlas of the cycling murine ovary. *Elife* **11**, e77239 (2022).
26. J. Zhou *et al.*, Dissecting the fate of Foxl2-expressing cells in fetal ovary using lineage tracing and single-cell transcriptomics. *Cell Discov* **8**, 139 (2022).
27. C. Mayère *et al.*, Origin, specification and differentiation of a rare supporting-like lineage in the developing mouse gonad. *Science advances* **8**, eabm0972 (2022).
28. J. E. Fortune, R. A. Cushman, C. M. Wahl, S. Kito, The primordial to primary follicle transition. *Mol. Cell. Endocrinol.* **163**, 53-60 (2000).

29. R. H. Rastetter *et al.*, Marker genes identify three somatic cell types in the fetal mouse ovary. *Developmental biology* **394**, 242-252 (2014).
30. L. Mork *et al.*, Temporal differences in granulosa cell specification in the ovary reflect distinct follicle fates in mice. *Biol. Reprod.* **86**, 37 (2012).
31. Z. Wang *et al.*, Follistatin288 Regulates Germ Cell Cyst Breakdown and Primordial Follicle Assembly in the Mouse Ovary. *PLoS ONE* **10**, e0129643 (2015).
32. C. Ahlmann-Eltze, W. Huber, glmGamPoi: fitting Gamma-Poisson generalized linear models on single cell count data. *Bioinformatics* **36**, 5701-5702 (2020).
33. J. Perez-Sanz *et al.*, Increased number of multi-oocyte follicles (MOFs) in juvenile p27Kip1 mutant mice: potential role of granulosa cells. *Human reproduction (Oxford, England)* **28**, 1023-1030 (2013).
34. X. Fan *et al.*, Single-cell reconstruction of follicular remodeling in the human adult ovary. *Nature communications* **10**, 3164 (2019).
35. Q. Li *et al.*, Genetic variations in the 3'-untranslated region of SLC18A2 are associated with serum FSH concentration in polycystic ovary syndrome patients and regulate gene expression in vitro. *Human reproduction (Oxford, England)* **31**, 2150-2157 (2016).
36. N. Gonen *et al.*, In vitro cellular reprogramming to model gonad development and its disorders. *Science advances* **9**, eabn9793 (2023).
37. H. Li *et al.*, p27(Kip1) directly represses Sox2 during embryonic stem cell differentiation. *Cell Stem Cell* **11**, 845-852 (2012).
38. I. Stevant *et al.*, Dissecting Cell Lineage Specification and Sex Fate Determination in Gonadal Somatic Cells Using Single-Cell Transcriptomics. *Cell reports* **26**, 3272-3283.e3273 (2019).
39. L. Garcia-Alonso *et al.*, Single-cell roadmap of human gonadal development. *Nature* **607**, 540-547 (2022).
40. K. Jagarlamudi, P. Reddy, D. Adhikari, K. Liu, Genetically modified mouse models for premature ovarian failure (POF). *Molecular and cellular endocrinology* **315**, 1-10 (2010).

41. B. Nicol *et al.*, Genome-wide identification of FOXL2 binding and characterization of FOXL2 feminizing action in the fetal gonads. *Human molecular genetics* **27**, 4273-4287 (2018).
42. S. Granados-Aparici *et al.*, SMAD3 directly regulates cell cycle genes to maintain arrest in granulosa cells of mouse primordial follicles. *Scientific reports* **9**, 6513 (2019).
43. H. Jakel, C. Weinl, L. Hengst, Phosphorylation of p27Kip1 by JAK2 directly links cytokine receptor signaling to cell cycle control. *Oncogene* **30**, 3502-3512 (2011).
44. K. Huang *et al.*, JAK signaling regulates germline cyst breakdown and primordial follicle formation in mice. *Biology Open* **7**, bio029470 (2018).
45. D. M. Maatouk, L. Mork, A. A. Chassot, M. C. Chaboissier, B. Capel, Disruption of mitotic arrest precedes precocious differentiation and transdifferentiation of pregranulosa cells in the perinatal Wnt4 mutant ovary. *Developmental biology* **383**, 295-306 (2013).
46. M. L. Fero *et al.*, A syndrome of multiorgan hyperplasia with features of gigantism, tumorigenesis, and female sterility in p27(Kip1)-deficient mice. *Cell* **85**, 733-744 (1996).
47. V. Moncho-Amor *et al.*, SOX2 is required independently in both stem and differentiated cells for pituitary tumorigenesis in p27 null mice. *bioRxiv* 10.1101/2020.06.09.142638, 2020.2006.2009.142638 (2020).
48. G. X. Y. Zheng *et al.*, Massively parallel digital transcriptional profiling of single cells. *Nat. Commun.* **8**, 14049 (2017).
49. T. Stuart *et al.*, Comprehensive Integration of Single-Cell Data. *Cell* **177**, 1888-1902.e1821 (2019).
50. B. Li, C. N. Dewey, RSEM: accurate transcript quantification from RNA-Seq data with or without a reference genome. *BMC Bioinformatics* **12**, 323 (2011).
51. A. Dobin *et al.*, STAR: ultrafast universal RNA-seq aligner. *Bioinformatics* **29**, 15-21 (2013).
52. D. S. DeLuca *et al.*, RNA-SeQC: RNA-seq metrics for quality control and process optimization. *Bioinformatics* **28**, 1530-1532 (2012).

53. M. I. Love, W. Huber, S. Anders, Moderated estimation of fold change and dispersion for RNA-seq data with DESeq2. *Genome Biol.* **15**, 550 (2014).
54. R. C. Development, Team, *R: A language and environment for statistical computing.* (R Foundation for Statistical Computing, Vienna, Austria, 2008).

Figure legends

Figure 1. Transcriptional profiling of whole ovaries before, during and after primordial follicle activation in the mouse.
(A) Diagram of the mouse ovary during late embryonic and early postnatal development, highlighting the key events of germ cell nest breakdown, primordial follicle formation and primordial follicle activation by timepoint. B) UMAP Dimensionality Reduction Plot showing individual cells coloured by cell type. Clusters are labelled by cell type. (C) Heatmap showing cluster markers in 5,000 cells.

Figure 2. A distinct gene expression signature in activating pregranulosa cells during primordial follicle activation.
(A) UMAP Dimensionality Reduction Plots showing individual cells from each individual timepoint coloured by cell type. (B) Dotplot showing the expression of the following genes associated with granulosa cells: *Amh, Amhr2, Cdkn1b, Esr2, Foxl2, Fst, Hmgcs2, Hsd17b1, Hsd3b1, Inha, Kitl, Nr5a2,* and *Runx1*. (C) Dotplot showing the expression of the following genes associated with proliferation: *mki67* and *Pcna*. (D) Heatmap showing distinct marker genes in granulosa cell clusters ranked by product of intensity x logFC. (E) Examples of 'switched on' genes. Schematic diagrams of early-stage follicles show the pregranulosa cells (pink) and granulosa cells (red) with the top marker genes that begin to be expressed in Gc_3 and Gc_4 at PND4 (novel genes in bold). Corresponding UMAPs for *Inha* and *Slc18a2* showing individual cell expression coloured in purple. (F) Examples of 'switched off' genes. Schematic diagrams of early-stage follicles show the dormant pregranulosa cells (orange) with the top marker genes that are expressed in Gc_1 and Gc_2 at E18.5

(novel genes in bold). Corresponding UMAPs for *Gng13* and *Myl9* showing individual cell expression coloured in purple.

Figure 3. Identification of p27-dependent elements of the distinct gene expression signature in activating pregranulosa cells during primordial follicle activation.
(A) Haematoxylin and Eosin (H&E) staining of PND8 ovaries in wild-type (WT) and *Cdkn1b*$^{-/-}$ mice. (B) Haematoxylin and Eosin (H&E) staining of E18.5 ovaries in wild-type (WT) and *Cdkn1b*$^{-/-}$ mice. (C) MA plot showing differential expression of gene transcripts between WT E18.5 and *Cdkn1b*$^{-/-}$ ovarian cells (upregulated genes in red, downregulated in blue, n = 4 replicates per group). Grey dots indicate genes below the $p \leq 0.05$ cutoff. (D) Heatmap showing differentially expressed genes in *Cdkn1b*$^{-/-}$ ovaries ($p \leq 0.05$) overlaid with granulosa cell subclustering analysis from the single-cell sequencing experiment (upregulated genes in red, downregulated genes in blue). Clusters and timepoints are labelled across the top of the heatmap and coloured according to the UMAP. (E) p27-dependent gene expression signature of activating pregranulosa cells. Schematic diagrams of early-stage follicles show the pregranulosa cells (pink) and granulosa cells (red). For example genes *Tnni3*, *Inha* and *Hsd3b1*, corresponding UMAPs and graphs of transcripts per million (TPM) expression in bulk RNA sequencing of E18.5 *Cdkn1b*$^{+/+}$ ovaries (white bar) and *Cdkn1b*$^{-/-}$ ovaries (red bar) shown.

FIGURE 1

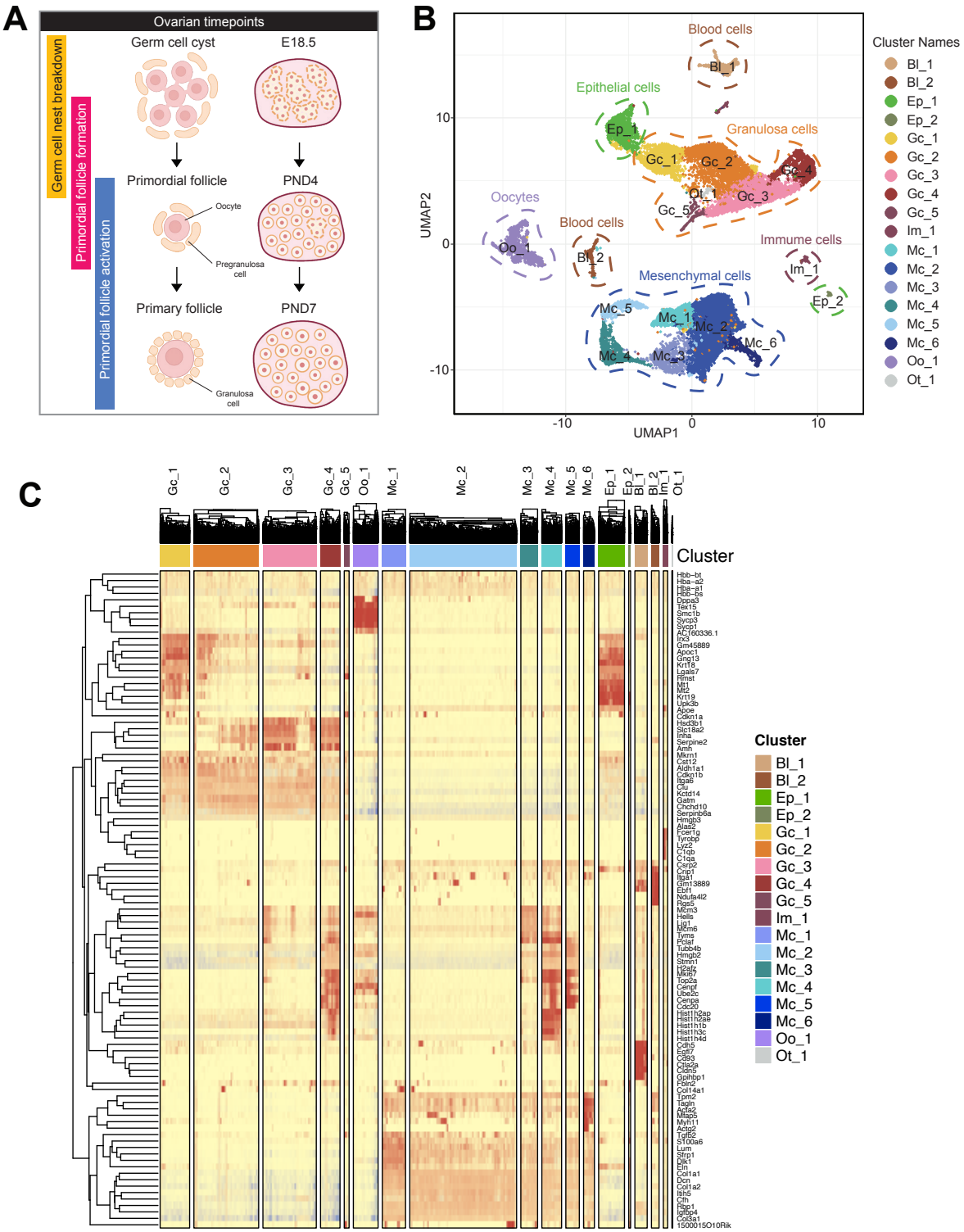
A
Ovarian timepoints
Germ cell nest breakdown
Primordial follicle formation
Primordial follicle activation
Germ cell cyst
E18.5
Primordial follicle
PND4
Oocyte
Pregranulosa cell
Primary follicle
PND7
Granulosa cell
B
Blood cells
Epithelial cells
Granulosa cells
Oocytes
Blood cells
Immune cells
Mesenchymal cells
UMAP2
UMAP1
Cluster Names
Bl_1
Bl_2
Ep_1
Ep_2
Gc_1
Gc_2
Gc_3
Gc_4
Gc_5
Im_1
Mc_1
Mc_2
Mc_3
Mc_4
Mc_5
Mc_6
Oo_1
Ot_1
C
Cluster

FIGURE 2

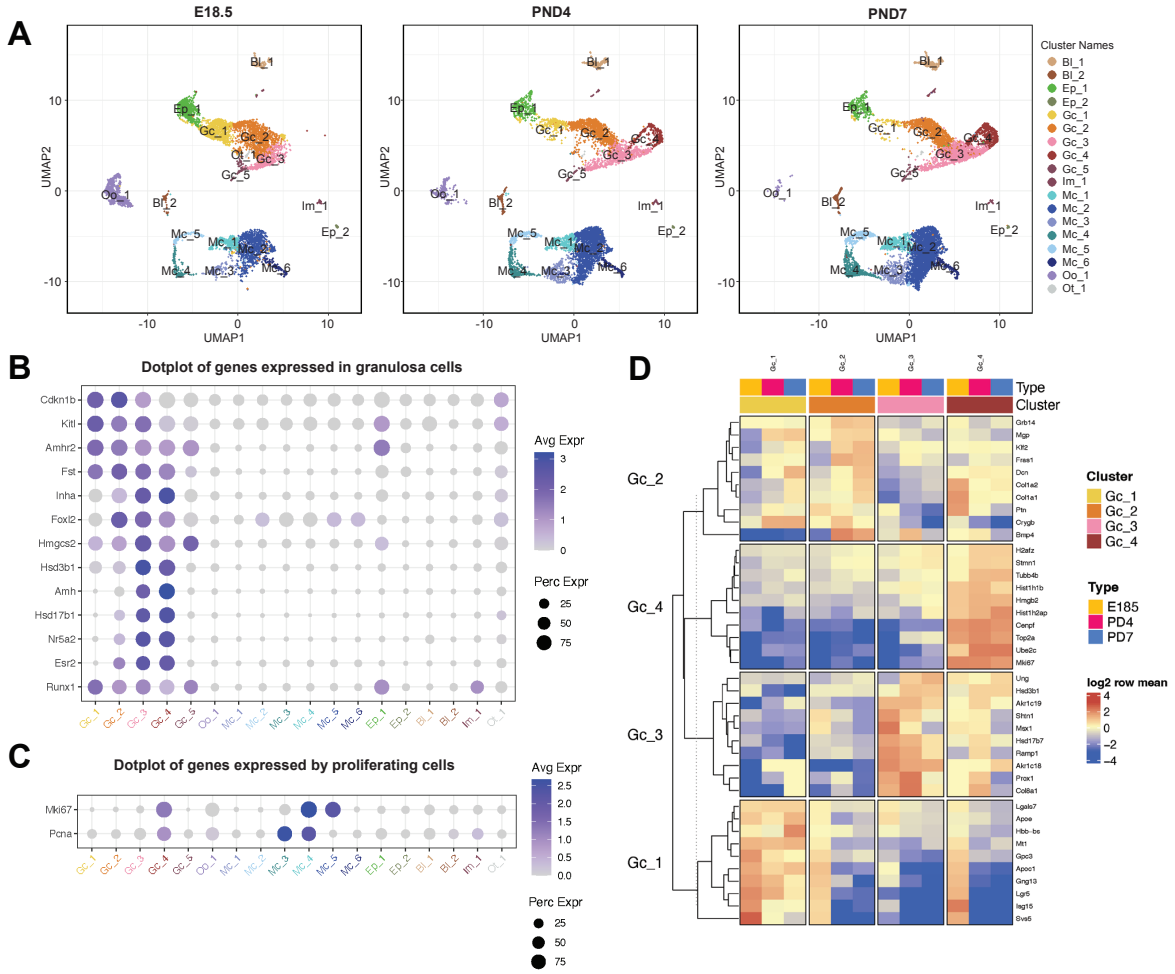
A
E18.5
PND4
PND7
UMAP1
UMAP2
Cluster Names
Bl_1
Bl_2
Ep_1
Ep_2
Gc_1
Gc_2
Gc_3
Gc_4
Gc_5
Im_1
Mc_1
Mc_2
Mc_3
Mc_4
Mc_5
Mc_6
Oo_1
Ot_1
B
Dotplot of genes expressed in granulosa cells
Cdkn1b
Kitl
Amhr2
Fst
Inha
Foxl2
Hmgcs2
Hsd3b1
Amh
Hsd17b1
Nr5a2
Esr2
Runx1
Avg Expr
Perc Expr
C
Dotplot of genes expressed by proliferating cells
Mki67
Pcna
D
Type
Cluster
Gc_2
Gc_4
Gc_3
Gc_1
Cluster
Gc_1
Gc_2
Gc_3
Gc_4
Type
E185
PD4
PD7
log2 row mean

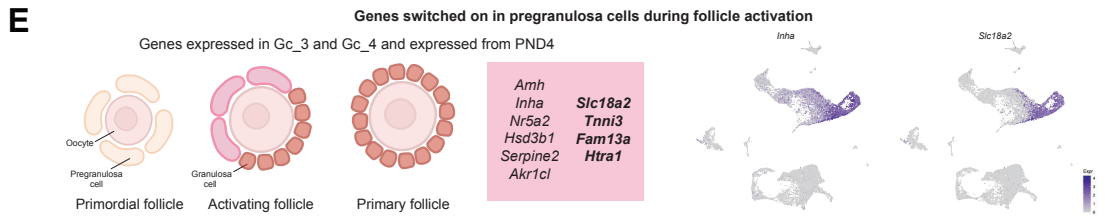
E
Genes switched on in pregranulosa cells during follicle activation
Genes expressed in Gc_3 and Gc_4 and expressed from PND4
Oocyte
Pregranulosa cell
Granulosa cell
Primordial follicle
Activating follicle
Primary follicle
Amh
Inha
Nr5a2
Hsd3b1
Serpine2
Akr1cl
Slc18a2
Tnni3
Fam13a
Htra1
Inha
Slc18a2

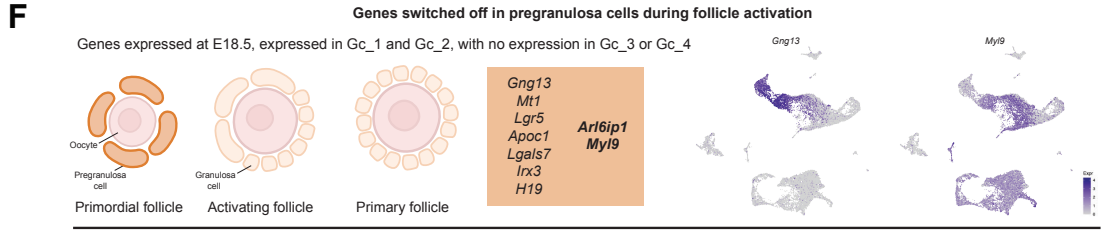
F
Genes switched off in pregranulosa cells during follicle activation
Genes expressed at E18.5, expressed in Gc_1 and Gc_2, with no expression in Gc_3 or Gc_4
Oocyte
Pregranulosa cell
Granulosa cell
Primordial follicle
Activating follicle
Primary follicle
Gng13
Mt1
Lgr5
Apoc1
Lgals7
Irx3
H19
Arl6ip1
Myl9
Gng13
Myl9

FIGURE 3

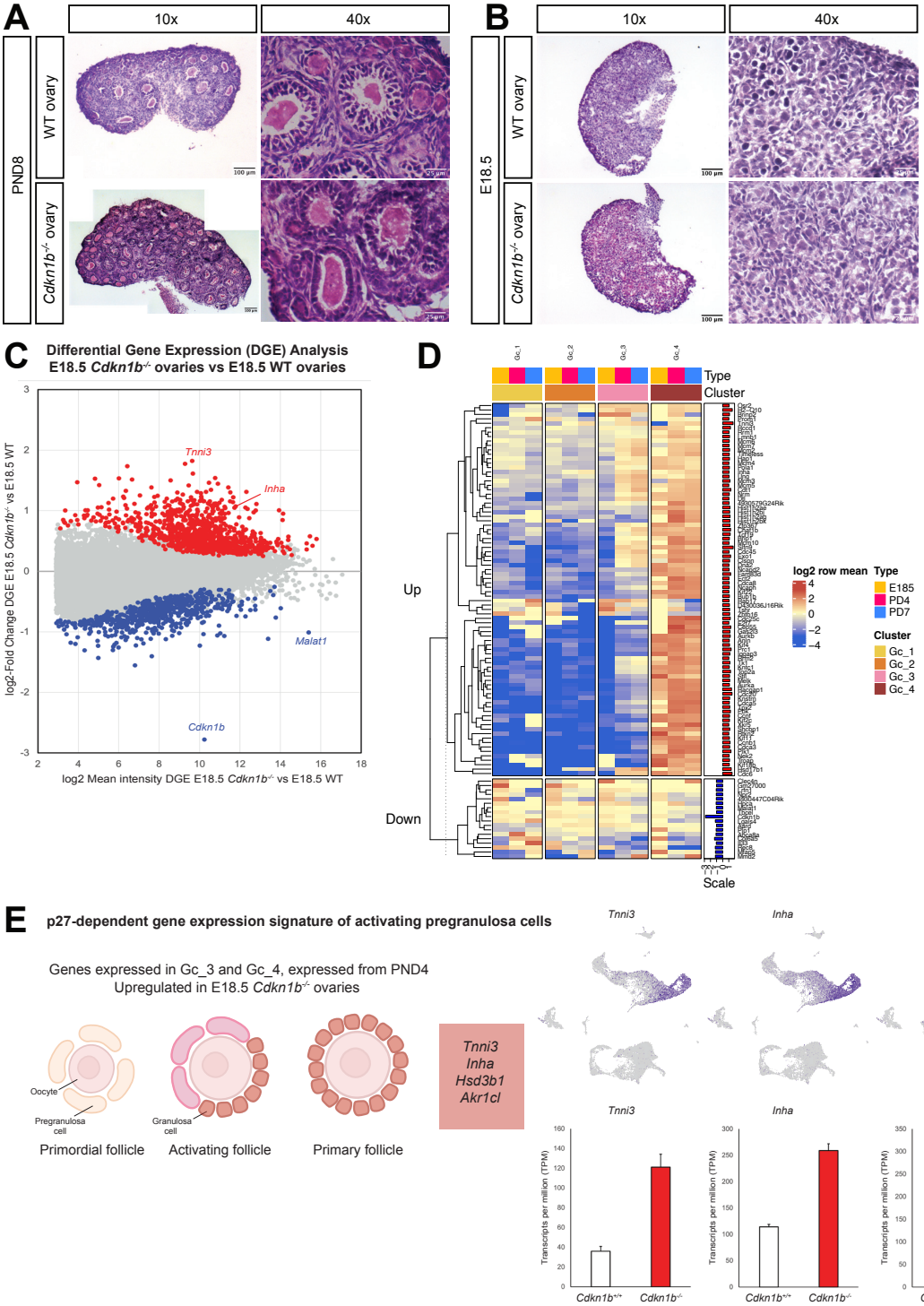
A
10x
40x
PND8
WT ovary
Cdkn1b-/- ovary
B
10x
40x
E18.5
WT ovary
Cdkn1b-/- ovary
C
Differential Gene Expression (DGE) Analysis
E18.5 Cdkn1b-/- ovaries vs E18.5 WT ovaries
Tnni3
Inha
Malat1
Cdkn1b
log2-Fold Change DGE E18.5 Cdkn1b-/- vs E18.5 WT
log2 Mean intensity DGE E18.5 Cdkn1b-/- vs E18.5 WT
D
Gc_1
Gc_2
Gc_3
Gc_4
Type
Cluster
Up
Down
Scale
log2 row mean
Type
E185
PD4
PD7
Cluster
Gc_1
Gc_2
Gc_3
Gc_4
E
p27-dependent gene expression signature of activating pregranulosa cells
Genes expressed in Gc_3 and Gc_4, expressed from PND4
Upregulated in E18.5 Cdkn1b-/- ovaries
Oocyte
Pregranulosa cell
Granulosa cell
Primordial follicle
Activating follicle
Primary follicle
Tnni3
Inha
Hsd3b1
Akr1cl
Tnni3
Inha
Hsd3b1
Transcripts per million (TPM)
Cdkn1b+/+
Cdkn1b-/-
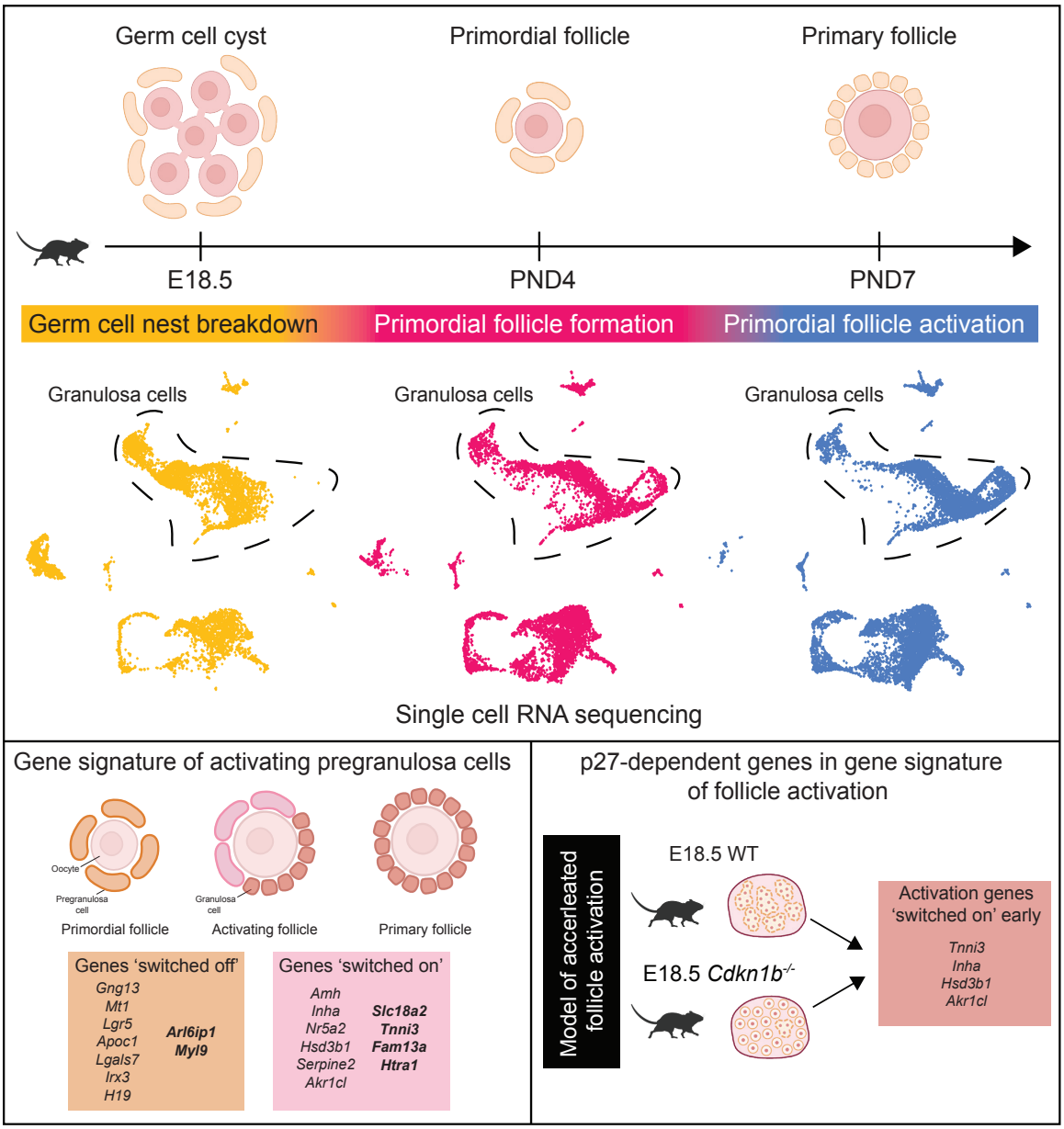
GRAPHICAL ABSTRACT